

# Chlorophyll Fluorescence Effects on Vegetation Apparent Reflectance: I. Leaf-Level Measurements and Model Simulation

Pablo J. Zarco-Tejada,<sup>\*</sup> John R. Miller,<sup>†</sup> Gina H. Mohammed,<sup>‡</sup>  
and Thomas L. Noland<sup>‡</sup>

**R**esults from a series of laboratory measurements of spectral reflectance and transmittance of individual leaves and from a modeling study are presented which demonstrate that effects of natural chlorophyll fluorescence (CF) are observable in the red edge spectral region. Measurements have been made with a Li-Cor Model 1800 integrating sphere apparatus coupled to an Ocean Optics Model ST1000 fiber spectrometer in which the same leaves are illuminated alternately with and without fluorescence-exciting radiation in order to separate the fluorescence emission component from the reflectance spectrum. The resulting difference spectrum is shown experimentally to be consistent with a fluorescence signature imposed on the inherent leaf reflectance signature. A study of the diurnal change in leaf reflectance spectra, combined with fluorescence measurements with the PAM-2000 Fluorometer, show that the difference spectra are consistent with observed diurnal changes in steady-state fluorescence. In addition, the time decay in the difference signature from repetitive leaf spectral reflectance measurements is seen to be consistent with the time decay of the leaf fluorescence signal (Kautsky effect) of dark-adapted leaves. The expected effects of chlorophyll fluorescence emission on the apparent spectral reflectance from a single leaf are also simulated theoretically using the doubling radiative transfer method.

These modeling results demonstrate that the laboratory observations of a difference spectrum with broad peak at about 750 nm and a much smaller peak near 690 nm are in agreement with theory. Model simulation shows that chlorophyll pigment and fluorescence each affect indices that are being used in optical remote sensing to characterize pigment levels and stress in vegetation canopies. Implications for high spectral resolution remote sensing of forest canopies are presented in a companion paper. ©2000 Elsevier Science Inc.

## INTRODUCTION

Experimental evidence of a solar-induced fluorescence signal superimposed on leaf reflectance signatures remains speculative. As a result of laboratory studies with a reflection-absorption-fluorescence spectrometer (VIRAF-spectrometer) (Buschmann and Lichtenthaler, 1988) concluded only that the detection of the effects of a fluorescence signal in the red edge reflective region (680–800 nm) cannot be excluded. Subsequently additional suggestions of the effect of fluorescence in apparent reflectance have been reported (Peñuelas et al., 1998; Gamon et al., 1997; Peñuelas et al., 1997; 1995; Gitelson et al., 1998; Gamon and Surfus, 1999). However, to the best of our knowledge, a quantitative demonstration of the effect of the fluorescence signal on the apparent reflectance spectra of leaves has remained unproven to date. The challenge has been to separate the effects of scattering and absorption within the leaf from the self-emission fluorescence processes.

The research reported in this article was motivated by a field experiment involving data acquisition with the Compact Airborne Spectrographic Imager (CASI) over 12 test sites of *Acer saccharum* M. (sugar maple) in which

<sup>\*</sup> Centre for Research in Earth and Space Science (CRESS), York University, Toronto, Canada

<sup>†</sup> Department of Physics and Astronomy, York University, Toronto, Canada

<sup>‡</sup> Ontario Forest Research Institute, Ontario Ministry of Natural Resources, Sault Ste. Marie, Ontario, Canada

Address correspondence to J. R. Miller, Centre for Research in Earth and Space Science (CRESS), York Univ., 4700 Keele St., Toronto, ON M3J 1P3, Canada. E-mail: pzarco@yorku.ca

Received 25 February 2000; revised 23 May 2000.

laboratory measurements of leaf samples of pigment content and chlorophyll fluorescence  $Fv/Fm$  using the PAM-2000 Fluorometer have shown the highest correlation between CASI forest canopy red edge indices and fluorescence indices (Zarco-Tejada et al., 1999a,b). These canopy results are discussed further in our companion paper (Zarco-Tejada et al., 2000). We have attempted to understand the basis for relationships observed between fluorescence measures and the passively observed above-canopy bidirectional reflectance.

Chlorophyll fluorescence (CF) is red and far-red light that is produced in plant photosynthetic tissues upon excitation with natural or artificial light in the visible spectrum. It emanates primarily from chlorophyll *a* in Photosystem II at room temperature. Production of CF is one of the ways in which plant chloroplasts harmlessly dissipate light energy that is in excess of the needs of photosynthesis, thereby, protecting the chloroplast from oxidative damage. Release of heat is the other, and more substantial, dissipation mechanism. Several reviews of CF theory, measurement methods and interpretation are available (e.g., Schreiber et al., 1994; Larcher, 1994; Lichtenthaler, 1992; Lichtenthaler and Rinderle, 1988; Schreiber and Bilger, 1987; Krause and Weis, 1984; Papageorgiou, 1975). In a general way, steady-state CF and photosynthetic rate are inversely related, such that CF is low when photosynthesis is high. However, CF can also decline when photosynthesis is low, because of an intensified protective quenching action on CF production, from heat dissipation. The interdependence of photosynthesis and CF, and the various mechanisms of CF quenching have been the subject of much research into the photobiology of a wide range of plant species (Govindjee, 1995; Mohammed et al., 1995; Larcher, 1994; Schreiber and Bilger, 1993; Lichtenthaler, 1992). Significantly, although leaf photosynthetic status as indicated by chlorophyll pigment content is a primary factor in determining leaf reflectance and transmittance spectra (e.g., Yamada and Fujimura, 1991; Jacquemoud et al., 1996) the leaf photosynthetic functioning as indicated by fluorescence emission is controlled by a wide range of factors in addition to leaf chlorophyll content, thereby underscoring the value in developing methods to estimate pigment levels in addition to measuring leaf fluorescence.

This article presents a simple technique for laboratory leaf measurements in which the fluorescence influence on the observed reflectance signature can be measured and are shown to be related to PAM-2000 fluorescence data from the same leaves. The response of this natural fluorescence signature has been studied with respect to the effect of the measurement technique, and in terms of its diurnal, pigment, and temporal variations supported by PAM-2000 fluorescence data. For comparison with the experimental data, a leaf radiative transfer model that includes fluorescence has been developed, based on the doubling method following Rosema et al. (1991), to permit the simulation of expected spectral fluorescence effects on the observed

leaf reflectance and transmittance spectra. Optical indices from the apparent reflectance spectra are proposed which are capable of tracking fluorescence in leaves.

## EXPERIMENTAL METHODS AND MATERIALS

Three-year-old potted trees of *Acer saccharum* M. (sugar maple) were used in the laboratory-greenhouse experiments of this study. Two experiments were designed to examine leaves with fixed pigment levels but under conditions in which fluorescence signals were expected to vary, in order to test whether experimental measurement methods presented were able to track such variations. Below we first describe the experimental procedures for the two experiments: diurnal fluorescence variations and time decay of fluorescence amplitude following light exposure. We then describe the detailed measurement methodologies employed in these experiments.

### Diurnal Variation Of Fluorescence

This study sampled 30 leaves which had similar chlorophyll content [49–53 units according to SPAD-502 (Minolta Camera Co., Ltd., Japan) chlorophyll *m* readings, and from subsequent pigment analysis,  $\bar{x}=58.08 \mu\text{g}/\text{cm}^2$ ,  $s=5.26$ ,  $n=30$ ]. Leaf samples were selected with similar chlorophyll content in order to study possible variations in the apparent leaf reflectance and transmittance due to normal diurnal changes of chlorophyll fluorescence.

The day before the experiment, leaves were selected and a circular area was marked on each leaf for subsequent sampling. On the morning of the study, trees were transferred from a shaded (50%) greenhouse environment to unshaded outdoor conditions at 0800 h, and returned to the greenhouse at 1430 h. This was done to induce a strong diurnal chlorophyll fluorescence response. Plants were sampled for chlorophyll fluorescence and spectral analysis at 07.00 h, 10.00 h, 13.00 h, 17.00 h, and 20.00 h.

At each sampling time, leaves (with petioles attached) were removed from the plants and immediately placed into plastic bags, sealed, and kept in a cooler on ice until one leaf had been sampled from each of six plants, typically <5 min collection time. They were taken into the laboratory, warmed briefly to room temperature, then sampled for effective quantum yield, then dark adapted for 30 min and re-sampled for  $Fv/Fm$  (as described below).

Measurements of reflectance and transmittance were made using the Li-Cor 1800 integrating sphere coupled to the 7.5 nm spectral resolution Ocean Optics ST1000 fiber spectrometer, and applying the methodology explained below which uses a long-pass optical filter to suppress excitation of Photosystem II (PSII) fluorescence signal from the apparent reflectance signal. These spectral readings were taken following the fluorescence measurement, allowing the calculation of the reflectance difference between the measurement with and without the long-pass filter (as described below).

Immediately after optical measurements were completed on each leaf, it was placed in a plastic bag, sealed and stored in the freezer for subsequent analysis of pigments.

### Time Decay Studies on Same Leaf

This experiment was designed to study the effects of fluorescence time decay on the measurements of apparent spectral reflectance. The leaf was inserted into the leaf holder in the Li-Cor apparatus and exposed to light for 5 min. Subsequently, leaf reflectance measurements were taken at 2 s intervals for 5 min, again with and then without the long-pass filter.

### Laboratory Measurement Methodologies

#### Chlorophyll Fluorescence

Chlorophyll fluorescence was analyzed with a Pulse Amplitude Modulation (PAM-2000) Fluorometer (Heinz Walz GmbH, Effeltrich, Germany), an instrument that has been used widely in basic and applied fluorescence research (Mohammed et al., 1995). Procedures used for measuring  $Fv/Fm$  and  $\Delta F/Fm'$  were based on standard methodologies as documented in the PAM-2000 manual (Heinz-Walz-GmbH, 1993).

The leaf was positioned in the PAM-2000 leaf clip holder, which exposes a sample area approximately 1 cm in diameter to the fiberoptic light emitter and detector array.

Steady-state fluorescence features were measured at 110 (Ft110) and 2820 (Ft2820)  $\mu\text{mol quanta m}^{-2} \text{s}^{-1}$  (supplied by a halogen light attachment, excitation wavelength  $<710 \text{ nm}$ ), to correspond to photosynthetic photon flux densities (PPFD) used in the reflectance and transmittance assessments (PPFD was monitored by a quantum sensor built into the leaf clip holder). Effective quantum yield, which denotes the actual efficiency of PSII photon capture in the light by closed PSII reaction centers, was determined as  $\Delta F/Fm' = (Fm' - Ft)/Fm'$ , where  $Fm'$  is the maximal fluorescence of a preilluminated sample with PSII centers closed and  $Ft$  is the fluorescence at steady-state (Genty et al., 1989; Van Kooten and Snel, 1990). The leaf was exposed to the PPFD for 2–3 s, then  $Ft$  was measured followed by  $Fm'$  upon application of a saturating pulse.

For measurement of maximal fluorescence induction, leaves were dark-adapted in the bags at room temperature for at least 30 min. Dark adaptation is necessary to oxidize electron carriers in the photosynthetic tissues, so that when the tissues are subsequently exposed to bright light, maximal fluorescence may be observed (Walker, 1985). The ratio of variable to maximal fluorescence  $Fv/Fm$  was determined for the adaxial (upper) leaf surface.  $Fv/Fm$  quantifies the maximal efficiency of photon capture by open PSII reaction centers (Butler and Kitajima, 1975), and is one of the most widely used chlorophyll fluorescence features (Mohammed et al., 1995). It is calculated from the equation  $Fv/Fm = (F_{\text{max}} - F_0)/F_{\text{max}}$ , where  $F_{\text{max}}$  is the maximal fluorescence yield of a dark-adapted sample, with all PSII reaction

centers fully closed, and  $F_0$  is the minimum fluorescence yield of a dark-adapted sample, with all PSII reaction centers fully open (Van Kooten and Snel, 1990).  $F_0$  is measured first, using a red measuring light with a maximum emission of 655 nm, at a very low PPFD of about 0.1  $\mu\text{mol quanta m}^{-2} \text{s}^{-1}$ , and a modulation frequency of 600 Hz.  $F_{\text{max}}$  was determined by exposing the sample to a saturating pulse of light ( $>6000 \mu\text{mol quanta m}^{-2} \text{s}^{-1}$ ,  $<710 \text{ nm}$  wavelength) of 0.8 s duration and 20 kHz modulation frequency. Fluorescence from the plant is detected at wavelengths  $>700 \text{ nm}$ . The instrument runs this test using an automated procedure and calculates the  $Fv/Fm$  ratio.

#### Apparent Leaf Reflectance and Transmittance Spectra

Single leaf reflectance and transmittance measurements were acquired on all leaf samples using a Li-Cor 1800-12 Integrating Sphere apparatus coupled by a 200  $\mu\text{m}$  diameter single mode fiber to an Ocean Optics Model ST 1000 spectrometer, with a 1024 element detector array, yielding a 0.5 nm sampling interval and  $\sim 7.3 \text{ nm}$  spectral resolution in the 340–860 nm range. The spectrometer is controlled and read out by a National Instruments multipurpose Data Acquisition Card (DAC-550). Software was designed to allow detailed control of signal verification, adjustment of integration time, and data acquisition (Harron and Miller, 1995). Spectral bandpass characterization performed using a mercury spectral line lamp source yielded full-width at half maximum (FWHM) bandwidth estimates of 7.37 nm, 7.15 nm, and 7.25 nm, at 438.5 nm, 546.1 nm and 576.9 nm respectively. Fiber spectrometer wavelength calibration was performed using the Ocean Optics HG-1 Mercury-Argon Calibration Source, that produces Hg and Ar emission lines between 253 nm and 922 nm.

Single leaf reflectance and transmittance measurements were acquired following the methodology described in the manual of the Li-Cor 1800-12 system (Li-Cor-Inc., 1983) in which six signal measurements are required: transmittance signal ( $TSP$ ), reflectance signal ( $RSS$ ), reflectance internal standard ( $RTS$ ), reflectance external reference ( $RST$ ), and dark measurements ( $TDP$ ,  $RSD$ ). Reflectance ( $Rfl$ ) and transmittance ( $Tns$ ) are calculated assuming a constant center wavelength and spectral bandpass [Eqs. (1) and (2)]. An integration time of 609.3 ms was used for all sample measurements.

$$Rfl = \frac{(RSS - RSD) \cdot Rfl_{\text{BaSO}_4}}{RTS - RSD}, \quad (1)$$

$$Tns = \frac{(TSP - TDP) \cdot Rfl_{\text{BaSO}_4}}{RST - RSD}, \quad (2)$$

with  $Rfl_{\text{BaSO}_4}$  the reflectance of barium sulfate.

A signal-to-noise study was carried out to choose the optimum function and bandwidth for the smoothing and derivative processing to be applied to the single leaf spectral reflectance and transmittance data prior to subsequent analysis and extraction of diagnostic indices.

A common method for smoothing and derivatives calculations (Savitzky and Golay, 1964) is based on a simplified polynomial least squares procedure, and has been widely adopted as evidenced by frequent reference in the literature (Enke and Nieman, 1976; Madden, 1978; Marchand and Marmet, 1983; Kawata and Minami, 1984; Demetriades-Shah et al., 1990; Tsai and Philpot, 1998). Other methods cited in the literature for smoothing purposes are: i) the moving-average filter, that uses a squared window as a filter; ii) a triangular function; and iii) an adaptive smoothing function (Kawata and Minami, 1984). Differentiation of spectra can be carried out by i) finite approximation difference, ii) linear regression derivative function; and iii) Savitzky–Golay derivative computation based on the simplified polynomial least square procedure mentioned before.

Based on the results of the SNR study for our experimental apparatus and samples, with very high sampling rate (small spacing) of the instrument, a very high frequency of the noise, and the relatively broad spectral features of leaf samples, Savitzky–Golay approach was selected with a third-order polynomial function with 25 nm bandwidth as optimum.

#### *Measurement Apparatus and Protocol for Distinguishing Fluorescence in Measurements of Apparent Spectral Reflectance*

The apparatus and methodology employed to measure the reflectance and transmittance spectra is based on the commercial Li-Cor Model 1800 integrating sphere system. A simple modification was made to the standard apparatus involving the purchase of a second Li-Cor Lamp/Collimator housing and the insertion of a Schott RG 695 colored long-pass glass filter at the exit aperture of one of the illuminator units. The Schott RG 695 colored glass filter, with 3 mm thickness, blocks radiant flux at  $\lambda < 695$  nm. As described below, with a suitable measurement protocol these two light sources enable reflectance and transmittance measurements of a given sample without fluorescence and including the effect of fluorescence. Using the “filtered illuminator” and standard illuminator in turn, reflectance and transmittance measurements were carried out on nonfluorescent (assured by the PAM-2000 Fluorometer) diffusing targets. Measurements showed that relative differences in reflectance and transmittance spectra for  $\lambda > 700$  nm, with and without the filter in the illuminator, were less than 2%. Photosynthetic photon flux density (PPFD) illumination values (measured with a Li-Cor quantum sensor) were  $110 \pm 2 \mu\text{mol m}^{-2} \text{s}^{-1}$  for the illuminator with the filter in and  $2820 \pm 5 \mu\text{mol m}^{-2} \text{s}^{-1}$  with no filter.

A set of 10 measurements per leaf sample were needed using the Li-Cor 1800 protocol to calculate leaf reflectance and transmittance with fluorescence signal embedded (no filter between target and light source) and without fluorescence signal (filter between target and light source). Leaf samples were dark-adapted before the measurements were carried out. The specific sequence of measurements with

the Li-Cor 1800 apparatus and fiber spectrometer and the two illuminators is provided in Table 1, and calculation of spectral reflectance and transmittance was determined from Eqs. (1) and (2). Measurements start with the filter between the leaf sample and the light source in order to substantially reduce the activation of PSII with visible light. No change in the position of the leaf sample was needed to proceed with the set of measurements without the filter. The measured leaf reflectance and transmittance with and without the filter can therefore be accurately compared in order to detect potentially-small differences due to a fluorescence signal.

A typical pair of reflectance spectra obtained with this measurement protocol is shown in Figure 1 illustrating the additive effect of the broad 740 nm fluorescence signal superimposed on the reflectance spectrum due only to the scattering and absorption effects within the leaf. Comparisons were considered valid for  $\lambda > 705$  nm due to the rapidly increasing noise level in the signal below that wavelength with the low Schott 695 filter transmission.

#### *Chlorophyll a and b and Total Carotenoids Content for Sugar Maple Leaves*

Leaves were stored at  $-23^\circ\text{C}$  until analysis. Two 2.3-cm circles were cut out of the leaf. One circle was ground in liquid  $\text{N}_2$ , weighed, and placed in a 15 mL centrifuge tube. The second circle was weighed, oven dried at  $80^\circ\text{C}$  for 24 h, and reweighed. Ten mL of *N,N*-dimethylformamide (spectralanalyzed grade, Fisher) was added to the tube. Tubes were placed horizontally in a darkened  $4^\circ\text{C}$  orbital shaker set to 100 rpm for 2 h to extract pigments, centrifuged at  $5^\circ\text{C}$  and 5000 g for 20 min, and placed in a dark,  $4^\circ\text{C}$  refrigerator for 20 min. Tubes were then removed from the refrigerator and 3 mL of supernatant removed and placed in a cuvette and the absorbance measured at 663.8 nm, 646.8 nm, and 480 nm with a Cary 1 spectrophotometer. Chlorophyll *a*, chlorophyll *b*, and total carotenoid concentrations were calculated using the extinction coefficients derived by (Wellburn, 1994).

## EXPERIMENTAL RESULTS

### **Diurnal Variation in Fluorescence**

Figures 2 and 3 show the diurnal variation of  $F_v/F_m$  and  $F_t110$ , respectively, observed during the day compared to the variation of the reflectance difference at 740 nm with and without the filter; therefore, tracking the PSII excitation to visible light superimposed on the reflectance when there is no excitation. The changes in the reflectance when there is visible excitation light are consistent and proportional to measurements of fluorescence in the leaf material. Results showed that variations in  $F_v/F_m$  during the day are captured in the leaf reflectance measurements even when the pigment concentration is constant.

Relationships were found between the observed reflectance difference at 740 nm ( $R_{diff@740\text{nm}}$ ) and  $F_v/F_m$

Table 1. Sequence of Measurements with the Li-Cor 1800 and Fiber Spectrometer To Enable the Calculation of Reflectance and Transmittance with Eqs. (1) and (2)<sup>a</sup>

Step	Setup	Lamp	Filter	White Plug	Dark Plug	Sample <sup>a,b,c</sup>	BaSO <sub>4</sub>
1	TSP	ON	IN	C	B	IN →	OUT
2	RSS	ON	IN	B	A	IN ←	OUT
3	RTS	ON	IN	C	A	IN ←	OUT
4	RSS	ON	OUT	B	A	IN ←	OUT
5	RTS	ON	OUT	C	A	IN ←	OUT
6	TSP	ON	OUT	C	B	IN →	OUT
7	RST	ON	OUT	B	A	OUT	IN
8	RST	ON	IN	B	A	OUT	IN
9	RSD	OFF	IN	B	A	OUT	OUT
10	TDP	OFF	IN	C	B	IN	OUT

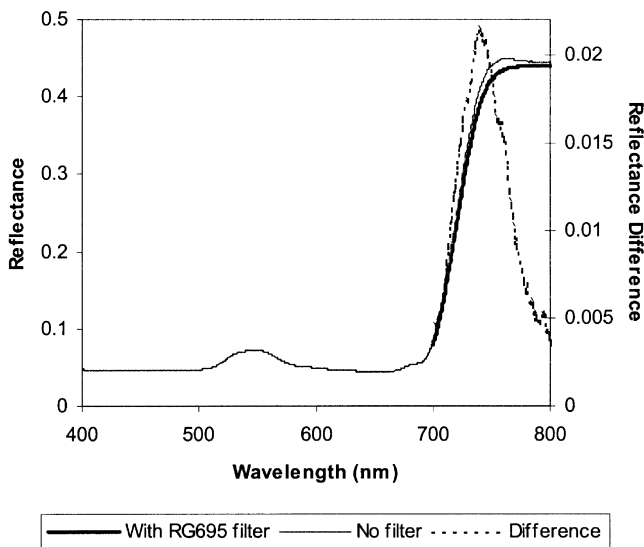
<sup>a</sup> Measurements start with the filter IN in order to substantially reduce the activation of PSII with visible light, with no change in the position of the leaf sample needed to proceed with the second set of measurements without the filter.

<sup>b</sup> IN →: adaxial leaf surface facing sample port A.

<sup>c</sup> IN ←: adaxial leaf surface facing sphere.

( $r^2=0.66$ , Fig. 4),  $F_{\text{MAX}}$  ( $r^2=0.62$ ),  $Ft110$  ( $r^2=0.54$ , Fig. 5),  $Ft2820$  ( $r^2=0.51$ ),  $Fm'2820$  ( $r^2=0.52$ ) which demonstrate the consistent relationships between spectral reflectance and CF features. The experiment shows that reflectance difference  $Rdiff@740\text{nm}$  tracks not only dark-adapted fluorescence ( $Fv/Fm$ ) but also steady-state fluorescence ( $Ft$  and  $Fm'$ ), and to lesser degree  $DF/Fm'$  ( $r^2=0.37$ ). In all cases, changes in CF in this experiment are due to fluorescence mechanisms alone since leaf chlorophyll content was selected to be effectively constant ( $\bar{x}=58.08 \mu\text{g}/\text{cm}^2$ ,  $s=5.26$ ,  $n=30$ ). Consequently, no relationship was expected or found between chlorophyll content and  $Rdiff@740\text{nm}$  ( $r^2=0.01$ ). Changes in  $R690$  were not-tested with this measurement

Figure 1. Single leaf reflectance measurements obtained with the Li-Cor 1800 apparatus and fiber spectrometer using the measurement protocol with the RG695 filter (thick line) and with no filter (thin line) from a dark-adapted *Acer saccharum* M. leaf sample. The additive effect of the broad 740 nm fluorescence signal super-imposed on the reflectance spectrum is shown.

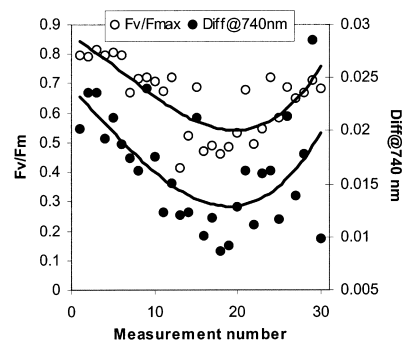


protocol because of the filter cutoff at 695 nm. Nevertheless, changes in that region are observed and are reported later in this article using optical indices related to changes in the reflectance curvature in the 680–690 nm region.

### Time Decay Studies on Same Leaf

Changes in CF amplitude subsequent to exposure were also tracked in apparent reflectance spectra. By exposing a dark-adapted leaf to sudden prolonged illumination, one can expect a classical Kautsky response pattern by which CF initially peaks then gradually decays in the ensuing minutes as a result of photochemical and nonphotochemical quenching of CF. This pattern, clearly evident in the CF measurements done with the Fluorometer, should also be discerned in reflectance difference patterns if fluorescence is affecting the apparent reflectance spectra. Mea-

Figure 2. Variation of  $Fv/Fm$  during the day of the experiment measured in leaf samples, compared to the variation of the reflectance difference at 740 nm ( $Rdiff@740$ ) with and without the filter. The similar tendencies in solid curves, which are the least-squares best fit through the two sets of data, show that the dark-adapted fluorescence is tracked by reflectance measurements.



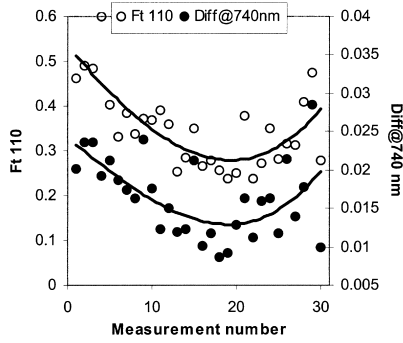


Figure 3. Variation of  $Ft_{110}$  during the day of the experiment measured in leaf samples, compared to the variation of the reflectance difference at 740 nm ( $R_{diff@740}$ ) with and without the filter. The similar tendencies in the solid curves, which are the least-squares best fit through the two sets of data, show that the steady-state fluorescence is tracked by reflectance measurements.

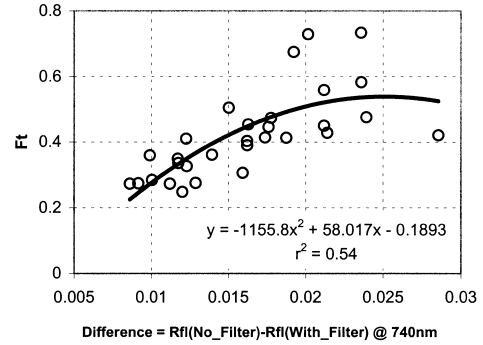


Figure 5. Relationship between steady-state fluorescence  $Ft_{110}$  and reflectance difference at 740 nm with and without the filter. Reflectance peak at 700–750 nm region is able to track changes in steady-state fluorescence features.

measurements were taken every 2 s during 5 min of illumination, alternating between with and then without the blocking filter. The comparison between the first and last spectral reflectance measurement made without the filter can be seen in Figure 6. The differences in apparent reflectance are easily seen in three spectral regions, with those at approximately 690 nm and 750 nm corresponding to the two chlorophyll fluorescence emission peaks. The other region, located near 370 nm in the blue, would not have originated from chlorophyll and needs further study. Figure 7 shows the change of the reflectance peak at 755 nm with time when the reflectance measurements made with and without filter are subtracted. The plot shows that the

time variation pattern is consistent with the Kautsky curve measured with the fluorometer.

### MODEL SIMULATION

#### Methodology

In the above experiments, chlorophyll fluorescence has been manipulated and the corresponding effects on apparent reflectance and transmittance measured. Another objective of our research is to determine whether these experimental results are theoretically consistent with natural fluorescence expected as a superimposed signal on the leaf reflectance and transmittance spectral signatures. Published leaf models such as PROSPECT (Jacquemoud and Baret, 1990) and Yamada and Fujimura (1991), which are both based on the earlier foundational work of Allen and Richardson (1968), have been used successfully to relate leaf biochemistry and scattering parameters to leaf reflectance and transmittance signatures. Although such models

Figure 4. Relationship between  $Fv/Fm$  and reflectance difference at 740 nm with and without the filter. Reflectance peak at 700–750 nm region is able to track changes in dark-adapted fluorescence  $Fv/Fm$ .

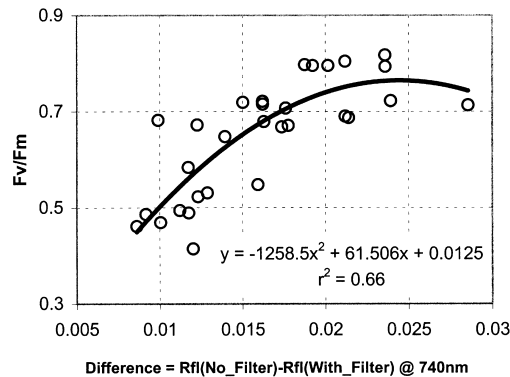
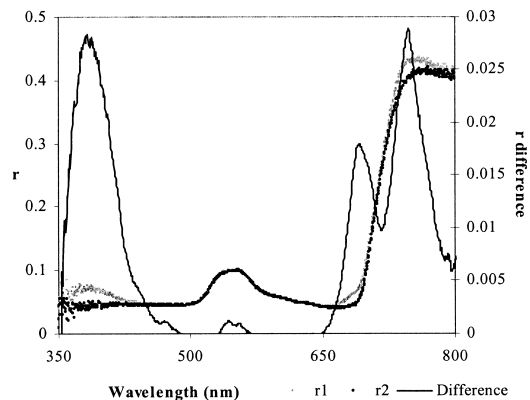


Figure 6. Reflectance measurements taken at  $t_0$  ( $r_1$ ) and  $t_1$  (5 min) ( $r_2$ ) which demonstrates that fluorescence emission bands affect the reflectance measurements.



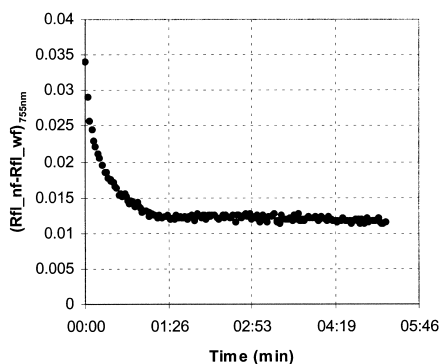


Figure 7. Variation of the reflectance difference at 755 nm with ( $Rfl\_wf$ ) and without filter ( $Rfl\_nf$ ) with time. It demonstrates the fluorescence decay at 755 nm with time after the illumination of a dark-adapted leaf.

provide convenient ways to characterize the leaf as a layered medium and the inherent optical absorption and scattering properties of the leaf, these models do not include the stimulation and flow of the fluorescence signal in the radiative transfer formulation. However, the models of Fukshansky and Kararinova (1980) and Rosema et al. (1991) are formulated specifically to include these effects. The former is focused on describing the effects within the leaf layers and the latter on simulating the effects of fluorescence effects in a plant canopy due to laser-induced fluorescence. For the purposes of this study, a simple leaf model has been constructed from some elements of the above models. Our measurements of leaf reflectance and transmittance without the influence of fluorescence stimulation can be exploited to provide a base set of leaf optical parameters from which the model can simulate the expected effects on apparent reflectance of varying fluorescence yield and chlorophyll pigment levels independently. The theoretical basis of the simulation approach is presented in Appendix A.

The model is based on Kubelka–Munk theory, modified following Fukshansky and Kazarinova (1980) to include fluorescence flux. The spectral character of fluorescence emission is based on Subhash and Mohanan (1997), described as two Gaussian emissions. The radiative transfer equations for a leaf layer are solved using the doubling method as in Rosema et al. (1991), extended to allow a description of expected fluorescence emission over the red edge region (650–800 nm region) resulting from stimulation by incident radiant flux over the entire PAR region. In order to make the simulation results applicable to the experimental measurements reported in this article, it was necessary to select leaf specific absorption and scattering properties that characterize the leaf material used in this study. Accordingly, the following simulation methodology was used.

Measurements of a single leaf reflectance and transmittance ( $r$ ,  $t$ ) without the effects of fluorescence stimula-

tion, as described above, form the basis for the derivation of the inherent scattering and absorption properties of the leaves under study. The matrix formulation, derived from Yamada and Fujimura (1991) as summarized in the Appendix, permits an individual leaf to be represented as a stack of three layers: a top epidermal layer, a compact inner layer containing the chloroplasts and cellular leaf material, and a lower epidermal layer. The two epidermal layers are assumed to contain no chlorophyll (although this is not strictly true) and to be defined solely in terms of their scattering properties as determined by the index of refraction. The tabulation in the PROSPECT model (Jacquemoud and Baret, 1990) is used to define the spectral behavior of the refractive index  $n_{e_i}$  of the epidermis. The corresponding reflectance and transmittance of the cuticular layer is then used to define the radiative transfer matrix  $\mathbf{G}_e$ , and the radiative transfer matrix of the leaf inner compact layer  $\mathbf{G}_I$  from Eqs. (A23) and (A24) in the Appendix. The corresponding inner leaf layer reflectance and transmittance is then calculated from Eq. (A25).

Now to simulate the radiation flow through a leaf the linear absorption and scattering coefficients ( $k$  and  $s$ ) of the leaf layers need to be specified. Furthermore, since in this simulation we wish to examine the leaf reflectance and fluorescence properties as a function of pigment concentration, a specific linear extinction coefficient is required. The extensive development and validation of the PROSPECT model (Jacquemoud and Baret, 1990; Jacquemoud et al., 1996) led us to adapt this formulation and the tabulated coefficient spectral values to our needs. Accordingly, for a leaf layer with total thickness  $D_L$ , the specific linear absorption coefficient ( $\text{mm}^{-1}$ ) at any wavelength can be expressed by the Eq. (3),

$$k = \gamma(\sum C_j K_j)/N \cdot D_L + k_e/D_L, \quad (3)$$

where  $C_j$  is the content of layer constituent  $j$  per unit area,  $K_j$  the corresponding specific absorption coefficient, and  $N$  the structure parameter from the PROSPECT model,  $k_e$  the residual absorption term attributed to the albino leaf, and  $\gamma$  is a factor which accounts for the variation in the coefficients with the diffuseness of the irradiance flow in the layer, with  $\gamma=1$  for perfectly diffuse light and  $\gamma=1/2$  for collimated light. This formulation allows the PROSPECT tabulations of  $K_j$  to be used for pigment, cellulose, lignin, protein and water, although only pigments are relevant to the spectral region in this study.

The selection of a specific linear scattering coefficient proved more problematic due to large differences in the spectral behavior of  $s$  reported in the literature. For example, the *in situ* fiber probe measurements of Fukshansky et al. (1991), the inversion results reported by Yamada and Fujimura (1991) and those of Rosema et al. (1991) show substantial differences, and, furthermore, require estimates of leaf thickness to be useful to the simulations of this study. Therefore, the equations in Allen and Richardson (1968) have been used to derive the Stokes parameters

from measured leaf layer reflectance and transmittance [Eq. (A26)], which in turn are used, with the measured leaf thickness, to compute the leaf layer Kubelka Munk linear scattering and extinction parameters  $k$  and  $s$ , according to Eqs. (A26) and (A27). This provided an effective method to obtain an estimate of the spectral behavior of the linear scattering coefficient. These derived parameters  $k$  and  $s$  were used to check that forward modeling could be used to retrieve the observed leaf reflectance and transmittance, and that the doubling method without fluorescence did in fact duplicate the results with the Kubelka Munk calculations. The result was a convenient leaf radiative transfer simulation model which includes both pigment content and fluorescence efficiency as independent input variables, with leaf scattering properties derived from sample leaves typical of the leaf samples under study. This simulation model then permitted a means for theoretical evaluation of the fluorescence signatures observed in the experimental portion of the study.

### Leaf Reflectance and Fluorescence Simulation Results

With the resulting fluorescence, reflectance and transmittance simulation model (FRT model) a wide range of experimental results can be simulated. First, with nominal leaf parameters the apparent reflectance with and without fluorescence can be simulated for qualitative comparison with the measurements reported earlier. Here we have used the leaf parameters: leaf thickness  $D=0.075$  mm, chlorophyll  $a+b$  content  $C=50 \mu\text{g}/\text{cm}^2$ , protein content ( $0.0012 \mu\text{g}/\text{cm}^2$ ) and cellulose plus lignin content ( $0.002 \text{g}/\text{cm}^2$ ), and PROSPECT structural parameter  $N=1.4$ . For the fluorescence signal we use Eq. (A3) with  $\lambda_L=690$  nm,  $\lambda_H=735$  nm,  $f_R=1$ ,  $\Delta_L=25$  nm,  $\Delta_H=60$  nm, and a fluorescence yield of 10% or 0% depending on whether the simulation is with, or without, fluorescence stimulation. The FRT model simulation results are shown in the Figure 8. It is clear from a comparison with the results reported above that the relative magnitudes of the fluorescence signature at 690 nm and 740 nm, and the deviations from the inherent reflectance signature that the observed signature is consistent with theory.

#### Model Assessment Using Experimental Data

The FRT model was tested using experimental leaf sample data described before. Chlorophyll fluorescence measurements for a constant pigment concentration data allowed the simulation of reflectance spectra. Comparison with leaf spectral reflectance measurements collected with and without the filter for non-fluorescence disturbance was performed.

The test was carried out using the data collected in the experiment where chlorophyll  $a+b$  contents were constant ( $\bar{x}=58.08 \mu\text{g}/\text{cm}^2$ ,  $s=5.26$ ,  $n=30$ ). Input parameters in the model were chl  $a+b$ ,  $F_v/F_m$  as fluorescence efficiency factor, measured with the PAM-2000, and leaf thickness. Results showed that peak at 700–750 nm region due

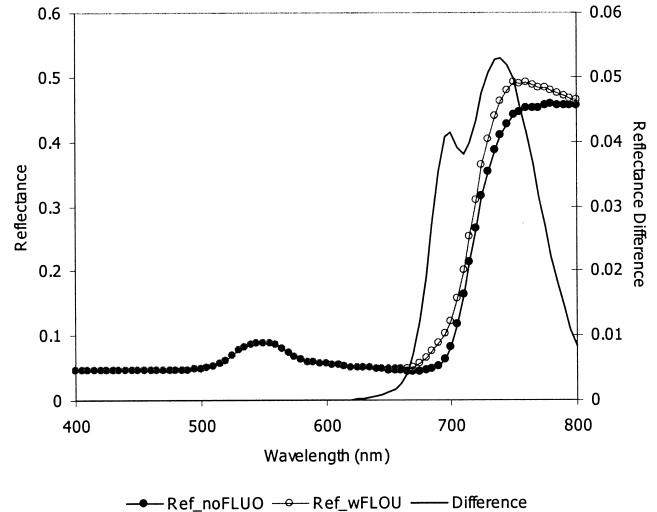


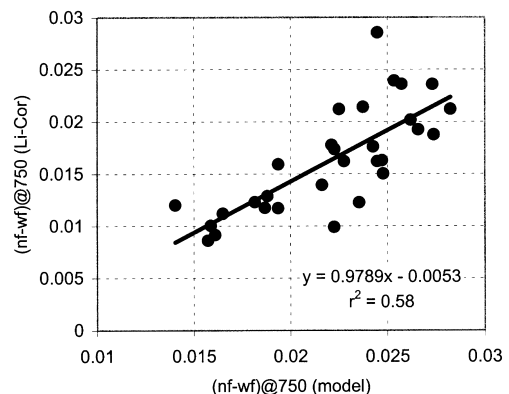
Figure 8. FRT Model simulating leaf reflectance with fluorescence (fluorescence efficiency=0.085, chl  $a+b$  content=50  $\mu\text{g}/\text{cm}^2$ , leaf thickness=0.075 mm, labeled as Ref\_wFLO), and without fluorescence (labeled as Ref\_noFLUO).

to fluorescence was tracked reasonably well by the model. Figure 9 shows that  $r^2=0.58$  was obtained in the comparison between the modeled  $R_{diff@750}$  and the real  $R_{diff@750}$  calculated from reflectance spectral measurements with the Li-Cor sphere with and without the filter.

The FRT model and the experiment with leaf samples with constant chlorophyll content allow us to look into optical indices that are able to track changes in reflectance due to chlorophyll fluorescence only, without being affected by chlorophyll content.

$R_{750}/R_{800}$  was calculated from leaf reflectance spectra with and without filter and studied for its relationship with fluorescence measurements: we see that the index

Figure 9. Peak at 750 nm due to fluorescence was tracked by the model. Relationship shows that  $r^2=0.58$  was obtained in the comparison between the  $R_{diff@750}$  predicted by the model and the real  $R_{diff@750}$  calculated from reflectance spectral measurements with the Li-Cor sphere with and without the filter.



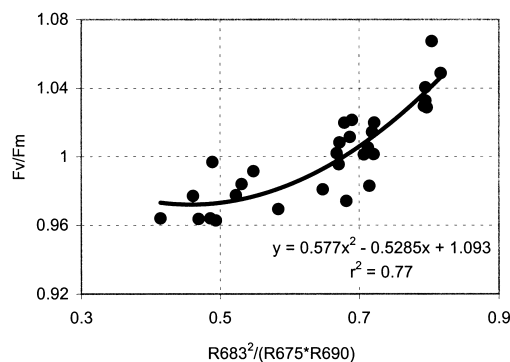


Figure 10. Relationship between the optical curvature index  $R683^2/R675 \cdot R691$  and  $Fv/Fm$ , from the experiment with maple leaves with constant chlorophyll content and diurnal variation of chlorophyll fluorescence.

tracks changes in  $CF$ , producing higher correlations when we use the data set with fluorescence signal ( $r^2=0.62$ , Yield110;  $r^2=0.51$ ,  $Ft110$ ;  $r^2=0.75$ ,  $Fv/Fm$ ). When we use the data without fluorescence the reflectance peak at 700–750 nm region disappears and the relationship with  $CF$  is removed ( $r^2=0.22$ , Yield110;  $r^2=0.18$ ,  $Ft110$ ;  $r^2=0.23$ ,  $Fv/Fm$ ). These results are consistent with the expected relationship between the reflectance peak in the region 700–750 nm and fluorescence measurements.

Reflectance changes in the 680–690 nm region can be studied with indices that are able to track the curvature of the reflectance spectrum, such as the curvature index  $R683^2/R675 \cdot R691$  that tracks changes centered at  $R683$ , therefore being affected by variations in reflectance due to  $CF$ . Results show that good relationships are found between the curvature index and  $CF$  measurements using data from the same experiment, where chlorophyll content was fixed:  $r^2=0.53$ , Yield110;  $r^2=0.65$ ,  $Ft110$ ;  $r^2=0.77$ ,  $Fv/Fm$  (Fig. 10). Other indices also result in high correlation with chlorophyll fluorescence, such as  $R685/R655$  ( $r^2=0.56$ , Yield110;  $r^2=0.75$ ,  $Ft110$ ;  $r^2=0.85$ ,  $Fv/Fm$ ),  $R690/R655$  ( $r^2=0.58$ , Yield110;  $r^2=0.76$ ,  $Ft110$ ;  $r^2=0.86$ ,  $Fv/Fm$ ). For constant chlorophyll content, these indices are therefore directly related only to chlorophyll fluorescence: consistently, no relationships were found between chlorophyll concentration and the reflectance indices  $R750/R800$  ( $r^2=0.19$ ), curvature ( $r^2=0.01$ ),  $R685/R655$  ( $r^2=0.005$ ), and  $R690/R655$  ( $r^2=0.002$ ).

A comparison between  $R750/R800$  and  $R683^2/R675 \cdot R691$  calculated from leaf reflectance spectra and simulated by the FRT model was performed (Figs. 11 and 12, respectively), with agreement between the predicted and measured optical index. Prediction errors are likely due to the model itself, which needs calibration of input parameters, as well as from experimental errors at the time of leaf reflectance measurements. Reflectance measurement duration time is also a critical factor that affects the reflectance peak at 700–750 nm region, due to rapid temporal

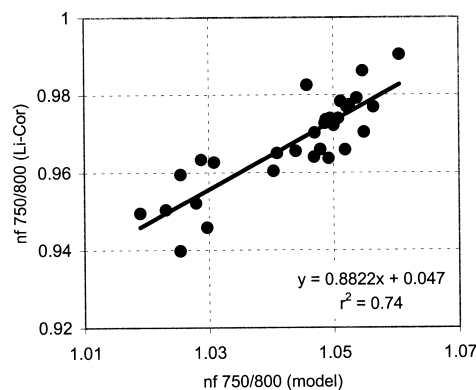


Figure 11. Relationship between the optical index  $R750/R800$  predicted by the FRT model and calculated from single leaf reflectance spectra.

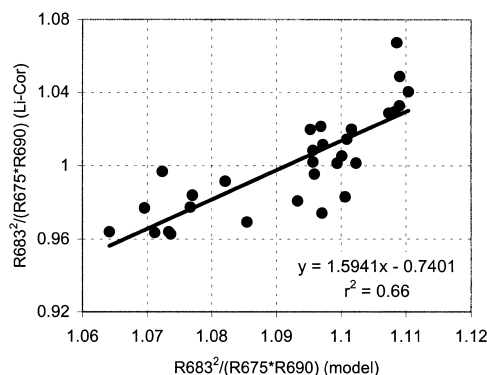
changes in chlorophyll fluorescence in dark-adapted leaf samples. Therefore, small differences in the time needed for single leaf measurement affects the amplitude of the reflectance peak and the optical index.

## DISCUSSION AND CONCLUSIONS

This article demonstrates quantitatively using both experimental and model simulation approaches that leaf apparent reflectance is affected by chlorophyll fluorescence. A set of laboratory experiments with *Acer saccharum* M. leaves permitted the collection of leaf reflectance and transmittance using a Li-Cor integrating sphere attached to a fiber spectrometer, as well as  $CF$  measurements using a PAM-2000 Fluorometer. A long-pass optical filter  $\lambda > 695$  nm placed between the light source and the leaf sample enabled the separation of reflectance and transmittance measurements without fluorescence and including the effect of fluorescence.

A diurnal experiment was carried out, keeping chloro-

Figure 12. Relationship between the curvature optical index  $R683^2/R675 \cdot R690$  predicted by the FRT model and calculated from single leaf reflectance spectra.



phyll content constant while  $CF$  was variable due to diurnal patterns. It showed that the reflectance difference at 740 nm followed the same pattern and correlated with  $Fv/Fm$  and steady-state fluorescence ( $r^2=0.66$ ,  $Fv/Fm$ ;  $r^2=0.54$ ,  $Ft$ ). A time-decay study using broad leaves illuminated for 5 min from a dark-adapted state showed differences in reflectance at 690 nm and 750 nm, corresponding to  $CF$  bands. The variation of apparent reflectance at 690 nm and 755 nm with time after exposure showed behavior similar to the Kautsky curve measured by the PAM-2000 Fluorometer.

The FRT (fluorescence–reflectance–transmittance) model, based on Kubelka Munk theory, modified to include the addition of fluorescence flux is presented in this article. It demonstrates that experimental results are theoretically consistent with  $CF$  expected as a superimposed signal on the leaf reflectance and transmittance spectral signatures. Model assessment shows that a theoretical basis exists for the relationships reported between  $CF$  and apparent reflectance at 690 nm and 750 nm. Reflectance differences at 750 nm calculated from leaves with constant chl  $a+b$  and variable  $CF$  showed good correlation with modeled spectra using  $Fv/Fm$  as fluorescence efficiency ( $r^2=0.58$ ).

The FRT model and the experiments with leaf samples with constant chl  $a+b$  permitted a validation of optical indices that can track changes of  $CF$  through reflectance. Indices associated to changes at 690 nm and 750 nm were tested, such as  $R750/R800$  ( $r^2=0.75$ ,  $Fv/Fm$ ), for which correlation degrades with leaf-measured  $CF$  when leaf reflectance without fluorescence is used ( $r^2=0.23$ ,  $Fv/Fm$ ). Indices in the 690 nm region showed good relationships with both dark-adapted  $Fv/Fm$  and steady-state fluorescence:  $R685/R655$  ( $r^2=0.85$ ,  $Fv/Fm$ ;  $r^2=0.75$ ,  $Ft$ );  $R690/R655$  ( $r^2=0.86$ ;  $Fv/Fm$ ;  $r^2=0.76$ ,  $Ft$ ); and a curvature index using the hyperspectral CASI sensor bandset in the 72-channel mode  $R683^2/[R675-R691]$  ( $r^2=0.77$ ,  $Fv/Fm$ ;  $r^2=0.65$ ,  $Ft$ ).

## APPENDIX: SIMULATION MODELING FOR RADIATIVE TRANSFER THROUGH A SINGLE LEAF: COMBINED REFLECTANCE, TRANSMITTANCE AND FLUORESCENCE UNDER BROADBAND ILLUMINATION

### Radiative Transfer Formulation, including Fluorescence, for a Leaf Layer

Based on Kubelka Munk theory, modified following Rosema et al. (1991) to include the addition of fluorescence flux  $F$ , the flow of total diffuse flux transmittance across a horizontal slab of thickness  $dz$  at any wavelength  $\lambda$  can be written in differential form as

$$\begin{aligned} -dT^-(z) &= -(k+s)(E^-(z)+F^-(z)) dz + s(E^+(z)+F^+(z)) \\ &\quad \times dz + 0.5P(z) dz, \\ dT^+(z) &= -(k+s)(E^+(z)+F^+(z)) dz + s(E^-(z)+F^-(z)) \\ &\quad \times dz + 0.5P(z) dz, \end{aligned} \quad (A1)$$

where

- $s$  is the linear back-scattering coefficient ( $\text{mm}^{-1}$ ) for diffuse light,
- $k$  is the linear absorption coefficient ( $\text{mm}^{-1}$ ) for diffuse light,
- $E^-(z)$  is the downward flowing illuminating irradiance at depth  $z$ ,
- $E^+(z)$  is the upward flowing, back-scattered, illuminating irradiance at depth  $z$ ,
- $F^-(z)$  is the downward fluorescence flux at depth  $z$ ,
- $F^+(z)$  is the upward fluorescence flux at depth  $z$ ,
- $T^-(z)=E^-(z)+F^-(z)$  is the total downward irradiance at depth  $z$ ,
- $T^+(z)=E^+(z)+F^+(z)$ , is the total upward irradiance at depth  $z$ ,
- $P(z)$  is the fluorescence emission flux at depth  $z$ , assumed to be isotropic,

which is defined as in Eq. (A2):

$$P(z) = \varphi \eta_i \int_{400}^{700} k(E^+(z)+E^-(z)) (\lambda/\lambda_{670}) d\lambda, \quad (A2)$$

where the integration is over the PAR spectral region,  $\varphi$  is the fraction of absorbed upward and downward illuminating PAR energy flux that contributes to fluorescence excitation, and  $\eta_i$  is the fluorescence emission spectral distribution function. The spectral character of  $\eta_i$  of fluorescence emission has been shown by Subhash and Mohanan (1997) to be effectively described as the sum of two Gaussian emissions with spectral peaks  $\lambda_L$  and  $\lambda_H$  at approximately 690 nm and 735 nm, respectively, with varying relative amplitudes. Accordingly, for the purposes of this simulation it is assumed that the spectral distribution of fluorescence can be expressed as

$$\eta_i = f_r \exp\left(\frac{-(\lambda-\lambda_L)^2}{a\Delta_L^2}\right) + \exp\left(\frac{-(\lambda-\lambda_H)^2}{a\Delta_H^2}\right), \quad (A3)$$

where  $f_r$  is the ratio of the fluorescence peak at  $\lambda_L$  relative to that at  $\lambda_H$ ,  $a$  is a Gaussian distribution constant equal to 0.3607, and  $\Delta_L$  and  $\Delta_H$  are the full-width at half maximum of the fluorescence emissions centered at  $\lambda_L$  and  $\lambda_H$ , respectively, with typical values of 25 nm and 80 nm (Subhash and Mohanan, 1997).

The doubling method, as described by Rosema et al. (1991), is a convenient approach for the description of the flow of illuminating flux and the excited fluorescence within individual leaf layers. Accordingly, the inherent reflectance  $r_i$ , transmittance  $t_i$ , and fluorescence  $f_i$  of the elementary leaf layer are defined as

$$\begin{aligned} r_i &= s_i dz, & t_i &= 1 - (k_i + s_i) dz, \\ \text{and} & & f_i &= \varphi \eta_i k_\pi (\lambda_\pi / \lambda) dz / 2, \end{aligned} \quad (A4)$$

where the  $\pi$  subscript refers to the average spectral value for the PAR light absorbing region. Accordingly, if two identical infinitesimally thin layers within the leaf layer are

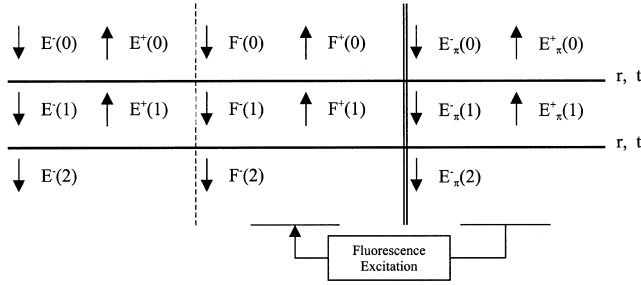


Figure 13. Schematic representation of the flow of irradiance for two elemental leaf layers.  $F$ ,  $E$ , and  $E\pi$  refer to fluorescence irradiance flux, irradiance, and irradiance in the PAR region, respectively. The superscripts + and - refer to up- and downward flowing flux. The reflectance and transmittance of the elemental layer within the leaf are  $r$  and  $t$ , respectively.

considered, the flux flow can be illustrated as shown in Figure 13.

Although the wavelength subscript for all spectral quantities is shown explicitly in the above equation to differentiate the absorbing PAR spectral region, for convenience it is omitted subsequently. Accordingly, the radiative transfer Eq. (A1) for an infinitesimal layer at any wavelength  $\lambda$  can be transformed using Eq. (A4) to yield the following sets of equations (after Rosema et al., 1991) for the three important fluxes through the two identical leaf layers in Figure 13:

(i) For the excitation fluxes in the PAR region [Eq. (A5)],

$$\begin{aligned} E_{\pi}^{-}(2) &= t_{D\pi} E_{\pi}^{-}(0) = x_{\pi} t_{\pi} E_{\pi}^{-}(0), \\ E_{\pi}^{+}(0) &= r_{D\pi} E_{\pi}^{-}(0) = r_{\pi} (1 + x_{\pi} t_{\pi}) E_{\pi}^{-}(0), \end{aligned} \quad (\text{A5})$$

where the double layer reflectance and transmittance in the excitation spectral region are given by

$$\begin{aligned} t_{D\pi} &= x_{\pi} t_{\pi}, \\ r_{D\pi} &= r_{\pi} (1 + x_{\pi} t_{\pi}), \end{aligned} \quad (\text{A6})$$

with [Eq. (A7)]

$$x_{\pi} = \frac{t_{\pi}}{(1 - r_{\pi} r_{\pi})} \quad (\text{A7})$$

and where  $r_{\pi}$  and  $t_{\pi}$  are the equivalent reflectance and transmittance of the elementary layer in the PAR region and  $r_{D\pi}$  and  $t_{D\pi}$  are the equivalent reflectance and transmittance in the PAR region of the doubled elementary layer. These fluxes contribute to the fluorescence at longer wavelength (660–800 nm).

(ii) For the incident irradiance flux at any wavelength  $\lambda$  [Eq. (A8)],

$$\begin{aligned} E^{-}(2) &= t_D E^{-}(0) = xt E^{-}(0) \\ E^{+}(0) &= r_D E^{-}(0) = r(1 + xt) E^{-}(0) \end{aligned} \quad (\text{A8})$$

where the double-layer transmittance and reflectance is

$$\begin{aligned} t_D &= xt \\ r_D &= r(1 + xt) \end{aligned} \quad (\text{A9})$$

with [Eq. (A10)]

$$x = \frac{t}{1 - r r} \quad (\text{A10})$$

(iii) For the fluorescence flux at wavelength  $\lambda$  greater than 660 nm [Eq. (A11)],

$$\begin{aligned} F^{-}(2) &= t_D F^{-}(0) + f_D E_{\pi}^{-}(0) \\ F^{+}(0) &= r_D F^{-}(0) + g_D E_{\pi}^{-}(0) \end{aligned} \quad (\text{A11})$$

where  $g_D$  and  $f_D$  are the front side and backside fluorescence response of the double layer to the flow of incident excitation flux in PAR region given by

$$\begin{aligned} g_D &= f(1 + x_{\pi} t + x_{\pi} r_{\pi} + xr) + xr x_{\pi} f(r + r_{\pi}), \\ f_D &= f(x + x_{\pi}) + x x_{\pi} f(r + r_{\pi}) \end{aligned} \quad (\text{A12})$$

with [Eq. (A13)]

$$x_{\pi} = \frac{t_{\pi}}{(1 - r_{\pi} r_{\pi})} \quad (\text{A13})$$

The recursion relations described by Eqs. (A6), (A9), and (A12) allow the optical properties of the double layer to be expressed in terms of the single layer. The irradiance and fluorescence fluxes can be simulated through an entire leaf layer (either the palisade or mesophyll layers or a single compact layer) by successive doublings, in which  $r_D$ ,  $t_D$ ,  $g_D$ , and  $f_D$  are substituted into the recursion equations for  $r$ ,  $t$ ,  $g$ , and  $f$ , and the new double layer  $E\pi$ ,  $E$ , and  $F$  fluxes are calculated. The number of doublings required depends on the layer thickness, with Rosema et al. (1991) suggesting 14 doublings for typical leaf dimensions.

### Single Leaf as a Stack of Layers

Whereas the above presents a convenient means of representing the flux flow across a leaf layer the epidermal layers are not explicitly included. Yamada and Fujimura (1991) have provided a convenient framework for the description of the flow of radiant fluxes across a dicotyledonous leaf. In this case the leaf was considered for simplicity as a stack of three layers, the upper epidermis, an active compact layer containing the chloroplasts and cells which give rise to the absorption, scattering and fluorescence, and the lower epidermal layer.

The total downward irradiance entering and the total upward irradiance emerging from above any layer or group of layers are designated  $T_a^{-}$  and  $T_a^{+}$ , respectively, whereas below this layer the total emerging downward irradiance and the total incident upward irradiance are designated  $T_b^{-}$  and  $T_b^{+}$ , respectively. Accordingly one can write the recursion relations for the flux across any layer  $k$ :

$$\begin{aligned} T_a^{+} &= r_a^{*} T_a^{-} + t_b^{*} T_b^{+}, \\ T_b^{-} &= t_a^{*} T_a^{-} + r_b^{*} T_b^{+}, \end{aligned} \quad (\text{A14})$$

where the layer (or group of layers) is defined by the apparent reflectance and transmittance coefficients,  $r_a^*$ ,  $r_b^*$ ,  $t_a^*$ , and  $t_b^*$ , with  $a$  denoting a view from the top and  $b$  denoting the view from the bottom. The designation “apparent” (denoted by the asterisk superscript for reflectance and  $t$ ) is required because the addition of fluorescence to the irradiance observed above and below the layer at wavelengths  $>660$  nm results in  $(r^*+t^*) > (r+t)$ , where the latter are the inherent layer reflectance and transmittance coefficients due to absorption and scattering alone; so, in fact, it is possible to have  $(r^*+t^*) > 1$ . Also, the upward and backward coefficients are, in general, not equal for an inhomogeneous layer or for a stack of different homogeneous layers, and is a well-known property for a dicotyledonous leaf.

For the  $i$ th layer in a leaf, or an arbitrary number of layers, Eqs. (A14) can be written in matrix form as Eqs. (A15) and (A16) (Yamada and Fujimura, 1991):

$$\begin{bmatrix} T_{bi}^- \\ T_{bi}^+ \end{bmatrix} = G_i \begin{bmatrix} T_{ai}^- \\ T_{ai}^+ \end{bmatrix}, \quad (\text{A15})$$

where

$$G_i = \frac{1}{t_{bi}^*} \begin{bmatrix} (t_{ai}^* t_{bi}^* - r_{ai}^* r_{bi}^*) & r_{bi}^* \\ -r_{ai}^* & 1 \end{bmatrix}, \quad (\text{A16})$$

which for a homogeneous layer reduces to Eq. (A17):

$$G_i = \frac{1}{t_i^*} \begin{bmatrix} (t_i^{*2} - r_i^{*2}) & r_i^* \\ -r_i^* & 1 \end{bmatrix}. \quad (\text{A17})$$

Therefore, for a three-layer model for a leaf the matrix radiative transfer equation becomes Eq. (A18):

$$\begin{bmatrix} T_3^- \\ T_3^+ \end{bmatrix} = \mathbf{G} \begin{bmatrix} T_1^- \\ T_1^+ \end{bmatrix}, \quad (\text{A18})$$

where

$$\mathbf{G} = \mathbf{G}_3 \mathbf{G}_2 \mathbf{G}_1. \quad (\text{A19})$$

Alternately, writing Eq. (A20), we obtain Eq. (A21):

$$\mathbf{G} = \begin{bmatrix} \mathbf{g}_{11} & \mathbf{g}_{12} \\ \mathbf{g}_{21} & \mathbf{g}_{22} \end{bmatrix}, \quad (\text{A20})$$

$$\begin{aligned} T_3^- &= g_{11} T_1^- + g_{12} T_1^+, \\ T_3^+ &= g_{21} T_1^- + g_{22} T_1^+. \end{aligned} \quad (\text{A21})$$

The above equations permit the definition of the apparent front and back leaf reflectance,  $\rho_a^*$  and  $\rho_b^*$ , respectively, and the apparent leaf transmittances  $\tau_a^*$  and  $\tau_b^*$ :

$$\begin{aligned} \rho_a^* &= -g_{21}/g_{22} & \text{and} & & \rho_b^* &= g_{12}/g_{22}, \\ \tau_a^* &= (g_{11}g_{22} - g_{12}g_{21})/g_{22} & \text{and} & & \tau_b^* &= 1/g_{22}. \end{aligned} \quad (\text{A22})$$

In order to simplify comparison between laboratory measurements and modeling, it is convenient to follow Yamada and Fujimura (1991) is defining the upper and lower cutic-

ular layers as equal with no pigment content, so that  $r_e = r_1 = r_3 = 1 - t_1 = 1 - t_3$ , where the reflectance of the epidermis  $r_e$  is defined only by its refractive index. Accordingly, the radiation transfer matrices for the cuticular layers are

$$G_e = G_3 = G_1 = \frac{1}{(1-r_e)} \begin{bmatrix} (1-2r_e) & r_e \\ -r_e & 1 \end{bmatrix}. \quad (\text{A23})$$

Following Yamada and Fujimura (1991), we note that the optical properties of the active layer of the leaf can be derived from measurements of the reflectance and transmittances of the entire leaf by noting that the radiation transfer matrix of the inside of the leaf is given by

$$G_l = G_e^{-1} G G_e^{-1}, \quad (\text{A24})$$

where  $G_e^{-1}$  denotes the inverse of the matrix  $G_e$ . The apparent reflectance and transmittances of the inside two active layers of the leaf are then from Eq. (A22):

$$\begin{aligned} r_{la}^* &= -g_{21}/g_{22}, \\ t_{la}^* &= (g_{11}g_{22} - g_{12}g_{21})/g_{22}. \end{aligned} \quad (\text{A25})$$

For this calculation of the inner layer reflectance and transmittance under the condition of no fluorescence stimulation, we get simply  $r$ ,  $t$ . Accordingly, these values can be related to leaf scattering and extinction properties of a compact leaf inner layer using Kubelka Munk radiative transfer theory. Allen and Richardson (1968) show that the corresponding Stokes parameters  $a$  and  $b$  are given by

$$\begin{aligned} a &= (1+r^2-t^2+\Delta)/2r, \\ b &= (1-r^2+t^2+\Delta)/2t, \end{aligned} \quad (\text{A26})$$

where

$$\Delta = \{(1+r+t)(1+r-t)(1-r+t)(1-r-t)\}^{1/2},$$

and the Kubelka Munk scattering and extinction parameters for the layer are

$$\begin{aligned} S &= \left[ \frac{2a}{(a^2-1)} \right] \log b, \\ K &= \left[ \frac{(a-1)}{(a+1)} \right] \log b, \end{aligned} \quad (\text{A27})$$

where division by the leaf layer thickness yields the linear scattering and extinction coefficients  $s$  and  $k$  used in Eq. (A1).

---

*The authors gratefully acknowledge the financial support provided for this research through the Centre for Research in Earth and Space Technology (CRESTech), the Ontario Ministry of Natural Resources, and GEOIDE (Geomatics for Informed Decisions) part of the Canadian Networks of Centres of Excellence program. Particular mention is also due to John Harron (CRESTech) for developments of the apparatus to perform single leaf measurements.*

## REFERENCES

- Allen, W. A., and Richardson, A. J. (1968), Interaction of light with a plant canopy. *J. Opt. Soc. Am.* 58:1023–1028.
- Buschmann, C., and Lichtenthaler, H. K. (1988), Reflectance and chlorophyll fluorescence signatures in leaves. In *Applications of Chlorophyll Fluorescence*, (H. K. Lichtenthaler, Ed.), Kluwer Academic, Dordrecht, pp. 325–332.
- Butler, W. L., and Kitajima, M. (1975), Fluorescence quenching in photosystem II of chloroplasts. *Biochim. Biophys. Acta* 376:116–125.
- Demetriades-Shah, T. H., Steven, M. D., and Clark, J. A. (1990), High resolution derivative spectra in remote sensing. *Remote Sens. Environ.* 33:55–64.
- Enke, C. G., and Nieman, T. A. (1976), Signal-to-noise ratio enhancement by least-squares polynomial smoothing. *Anal. Chem.* 48:705A–712A.
- Fukshansky, L., and Kararino, N. (1980), Extension of the Kubelka-Munk theory of light propagation in the intensely scattering materials to fluorescent materials. *J. Opt. Soc. Am.* 70:1101–1111.
- Fukshansky, L., Fukshansky-Kazarinova, N., and Remisowsky, A. M. V. (1991), Estimation of optical parameters in a living tissue by solving the inverse problem of the multiflux radiative transfer. *Appl. Opt.* 30:3145–3153.
- Gamon, J. A., Serrano, L., and Surfus, J. S. (1997), The photochemical reflectance index: an optical indicator of photosynthetic radiation-use efficiency across species, functional types, and nutrient levels. *Oecologia* 112:492–501.
- Gamon, J. A., and Surfus, J. S. (1999), Assessing leaf pigment content and activity with a reflectometer. *New Phytol.* 143:105–117.
- Genty, B., Briantais, J. M., and Baker, N. R. (1989), The relationship between the quantum yield of photosynthetic electron transport and quenching of chlorophyll fluorescence. *Biochim. Biophys. Acta* 990:87–92.
- Gitelson, A. A., Stark, R., Kaufman, Y., and Merzlyak, M. (1998), Remote sensing techniques for estimation of pigment content in higher plants. In *First International Conference on Geospatial Information in Agriculture and Forestry*, Lake Buena Vista, FL, pp. II-545–II-546.
- Govindjee (1995), Sixty-three years since Kautsky: chlorophyll a fluorescence. *Aust. J. Plant Physiol.* 22:131–160.
- Harron, J. W., and Miller, J. R. (1995), An alternate methodology for reflectance and transmittance measurements of conifer needles. In *17th Canadian Symposium on Remote Sensing*, Saskatoon, Saskatchewan, Vol. II, pp. 654–661.
- Heinz-Walz-GmbH (1993), Portable Fluorometer PAM-2000 and data acquisition software DA-2000, Effeltrich, Germany.
- Jacquemoud, S., and Baret, F. (1990), Prospect: a model of leaf optical properties spectra. *Remote Sens. Environ.* 34:75–91.
- Jacquemoud, S., Ustin, S. L., Verdebout, J., Schmuck, G., Andreoli, G., and Hosgood, B. (1996), Estimating leaf biochemistry using the PROSPECT leaf optical properties model. *Remote Sens. Environ.* 56:194–202.
- Kawata, S., and Minami, S. (1984), Adaptive smoothing of spectroscopic data by a linear mean-square estimation. *Appl. Spectrosc.* 38:49–58.
- Krause, G. H., and Weis, E. (1984), Chlorophyll fluorescence as a tool in plant physiology. II. Interpretation of fluorescence signals. *Photosynthesis Res.* 5:139–157.
- Larcher, W. (1994), Photosynthesis as a tool for indicating temperature stress events. In *Ecophysiology of Photosynthesis* (E. D. Schulze and M. M. Caldwell, Eds.), Springer-Verlag, Berlin, pp. 261–277.
- Lichtenthaler, H. K. (1992), The Kautsky effect: 60 years of chlorophyll fluorescence induction kinetics. *Photosynthetica* 27:45–55.
- Lichtenthaler, H. K., and Rinderle, U. (1988), The role of chlorophyll fluorescence in the detection of stress conditions in plants. *CRC Crit. Rev. Anal. Chem.* 19(Suppl. 1):529–585.
- Li-Cor Inc. (1983), 1800–12 Integrating Sphere Instruction Manual, Publication No. 8305–0034.
- Madden, H. H. (1978), Comments on the Savitzky-Golay convolution method for least-squares fit smoothing and differentiation of digital data. *Anal. Chem.* 50:1383–1386.
- Marchand, P., and Marmet, L. (1983), Binomial smoothing filter: a way to avoid some pitfalls of least-squares polynomial smoothing. *Rev. Sci. Instrum.* 54:1034–1041.
- Mohammed, G. H., Binder, W. D., and Gillies, S. L. (1995), Chlorophyll fluorescence: A review of its practical forestry applications and instrumentation. *Scand. J. For. Res.* 10:383–410.
- Papageorgiou, G. (1975), Chlorophyll fluorescence: an intrinsic probe of photosynthesis. In *Bioenergetics of Photosynthesis* (Govindjee, Ed.), Academic, New York, pp. 319–371.
- Peñuelas, J., Filella, I., Lloret, P., Muñoz, F., and Vilajeliu, M. (1995), Reflectance assessment of mite effects on apple trees. *Int. J. Remote Sens.* 16:2727–2733.
- Peñuelas, J., Llusia, J., Piñol, J., and Filella, I. (1997), Photochemical reflectance index and leaf photosynthetic radiation-use efficiency assessment in Mediterranean trees. *Int. J. Remote Sens.* 18:2863–2868.
- Peñuelas, J., Filella, I., Llusia, J., Siscart, D., and Pinol, J. (1998), Comparative field study of spring and summer leaf gas exchange and photobiology of the mediterranean trees *Quercus ilex* and *Phillyrea latifolia*. *J. Exp. Bot.* 49:229–238.
- Rosema, A., Verhoef, W., Schroote, J., and Snel, J. F. H. (1991), Simulating fluorescence light-canopy interaction in support of laser-induced fluorescence measurements. *Remote Sens. Environ.* 37:117–130.
- Savitzky, A., and Golay, M. J. E. (1964), Smoothing and differentiation of data by simplified least squares procedures. *Anal. Chem.* 36:1627–1639.
- Schreiber, U., and Bilger, W. (1987), Rapid assessment of stress effects on plant leaves by chlorophyll fluorescence measurements. In *Plant Response to Stress* (J. D. Tenhunen and E. M. Catarino, Eds.), Springer-Verlag, Berlin, pp. 27–53.
- Schreiber, U., and Bilger, W. (1993), Progress in chlorophyll fluorescence research: major development during the past years in retrospect. *Prog. Bot.* 54:151–173.
- Schreiber, U., Bilger, W., and Neubauer, C. (1994), Chlorophyll fluorescence as a non-destructive indicator for rapid assessment of in vivo photosynthesis. *Ecol. Stud.* 71:49–70.
- Subhash, N., and Mohanan, C. N. (1997), Curve-fit analysis of chlorophyll fluorescence spectra: Application to nutrient stress detection in sunflower. *Remote Sens. Environ.* 60:347–356.
- Tsai, F., and Philpot, W. (1998), Derivative analysis of hyperspectral data. *Remote Sens. Environ.* 66:41–51.
- Van Kooten, O., and Snel, J. F. H. (1990), The use of chlorophyll fluorescence nomenclature in plant stress physiology. *Photosynthesis Res.* 25:147–150.
- Walker, D. A. (1985), Measurement of oxygen and chlorophyll

- fluorescence. In *Techniques in Bioproductivity and Photosynthesis* (J. Coombs, D. O. Hall, S. P. Long, and J. M. O. Scurlock, Eds.), Pergamon, Toronto, pp. 95–106.
- Wellburn, A. R. (1994), The spectral determination of chlorophylls a and b, as well as total carotenoids using various solvents with spectrophotometers of different resolutions. *J. Plant Physiol.* 144:307–313.
- Yamada, N., and Fujimura, S. (1991), Nondestructive measurement of chlorophyll pigment content in plant leaves from three-color reflectance and transmittance. *Appl. Opt.* 30: 3964–3973.
- Zarco-Tejada, P. J., Miller, J. R., Mohammed, G. H., Noland, T. L., and Sampson, P. H. (1999a), Canopy optical indices from infinite reflectance and canopy reflectance models for forest condition monitoring: application to hyperspectral CASI data. In *IEEE 1999 International Geoscience and Remote Sensing Symposium, IGARSS'99*, Hamburg (Germany).
- Zarco-Tejada, P. J., Miller, J. R., Mohammed, G. H., Noland, T. L., and Sampson, P. H. (1999b), Optical indices as bioindicators of forest condition from hyperspectral CASI data. In *Proceedings 19th Symposium of the European Association of Remote Sensing Laboratories (EARSeL)*, Valladolid (Spain).
- Zarco-Tejada, P. J., Miller, J. R., Mohammed, G. H., Noland, T. L., and Sampson, P. H. (2000), Chlorophyll fluorescence effects on vegetation apparent reflectance: II. Laboratory and airborne canopy-level measurements with hyperspectral data. *Remote Sens. Environ.* 74:596–608.